Effects of the presence of free lime nodules into concrete: experimentation and modelling

Luc COURARD*, Hervé DEGEE, Anne DARIMONT

University of Liege, Department of Architecture, Geology, Environment and Constructions, Belgium

ABSTRACT

When nodules of lime are embedded into concrete, the expansion accompanying the transformation of CaO into $Ca(OH)_2$ induces stresses and strains in both the lime nodule and in the concrete matrix. The concrete cover thickness, the diameter and the shape of the lime nodule as well as the mechanical characteristics of concrete and lime are the key parameters influencing the development of internal pressure and hence controlling the risk of cracking or pop-out. In order to study the effect of lime into cementitious concretes, laboratory investigations and modelling have been performed and show that the minimum cover thickness necessary to avoid the development of the pop-out phenomenon is estimated of the order of half the diameter of the inclusion. This is coming from the observation that expansion happens inside the porosity of the hydrated lime $Ca(OH)_2$: ESEM and DRX analysis confirm the effect of confinement in the development of crystals.

University of Liège, Civil and Mechanical Engineering Institute (B 52/3). Chemin des Chevreuils, 1, B - 4000 LIEGE, Belgium – Phone: 32.4.366.93.50 – Fax: 32.4.366.92.38 – Email: Luc.Courard@ulg.ac.be

Keywords: hydration, mechanical properties, CaO, concrete, pop-out.

1. Introduction

Lime has been used for a very long time in construction and buildings: Roman cement was already made of a part of lime while it remained the only binder used until modern cement were designed during XIXth century [1]. Lime is an industrial product obtained by calcination of limestone in a lime kiln [2]. This is described as a *bright lime* (Table 1), because of its high reactivity with water. The bulk density of the limestones industrially used for the manufacture of lime usually offers a lower density than calcite used for ornamental stones: porosity maybe up to 30% [3]. Quick lime is very reactive with water and hydrates are quickly formed [4]. Hydration process is accompanied by a significant proliferation (Table 1). The formation of $Ca(OH)_2$ yields in larger volume (expansive reaction). The ratio of volume change from CaO particle to $Ca(OH)_2$ is $33.1/16.8 \approx 2$.

Table 1

Hydration of quick to hydrated lime [2, 3].

Property	**CaO**	**+ H_2O**	**→ $Ca(OH)_2$**
Molecular weight	56.08	18.01	74.09
Bulk density (g/cm^3)	1.40 -1.90		0.45 -0.65
Specific density (g/cm^3)	3.33	1	2.24
Molar volume (cm^3/mole)	56.08/3.33=**16.8**		74.09/2.24 = **33.1**

The doubling of the molar volume (from 16.8 to 33.1 cm^3/mole) is responsible for expansion during hydration [4]. The intensity and speed of hydration are governed by lime purity, particle size, surface area, ...etc [5]. Burning temperature and kiln technology are also two important discriminant factors in the case of industrial lime production [3].

An interesting parameter used to quantify the reactivity of lime is the so-called T60, which is measured in accordance with standardized method EN 459-2:2001. It gives the speed of lime extinction, or the time needed to attempt a temperature of 60°C: the smaller it is, the more reactive the lime is. In some cases, the lime can be dead burned, leading to high density CaO grains. [4]. This dead burn lime hydrates very slowly because of a reduced porosity [6]. When lime is incorporated into concrete, problems due to expansion may occur (Fig.1): this phenomenon is well known as *pop-out* [7, 8, 9, 10, 11].

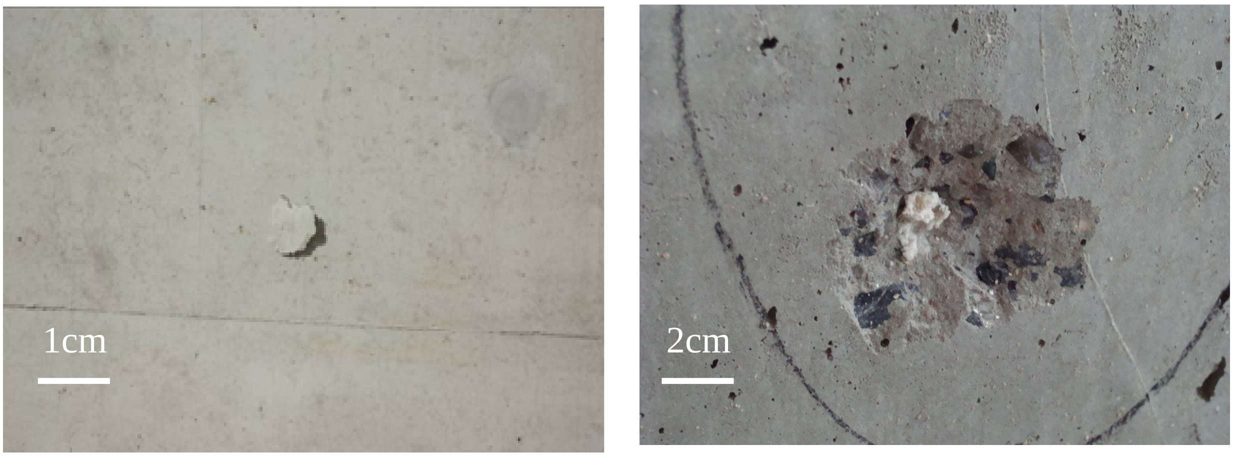

Fig. 1. Degradations induced by *pop-out* in concrete.

In many cases, quick lime is present in steel or iron slags [8, 9]. That means that it is rarely in the form of millimeter-sized aggregate in a confined environment. In the case of steel slags, Deng et al. [10] observed that expansion rates are depending on the type of cement and the percentage of lime: for lime contents of 2 and 5% (by weight of cement), the maximum observed rate of expansion is 0.12 and 0.7%, respectively, for cement type CEM I. The expansion force is estimated at 11.87 MPa at 3 days. A “dead” lime was used for experimentation and required alkali activation: the concentration of OH-ions in the pore solution of cement paste controls the expansion by affecting the positions occupied by the crystals of $Ca(OH)_2$ and the pressure of crystallization. Analyzes of the behaviour of LD steel slags containing lime nodules [11] were also conducted as a result of damage observed. An expansion rate of 0.16% (measured by immersion according to the Korean standard KS F 2580) was considered. The finite element calculations show that the depth of the pop-out increases as concrete strength decreases and the diameter of the slag increases (Fig. 2).

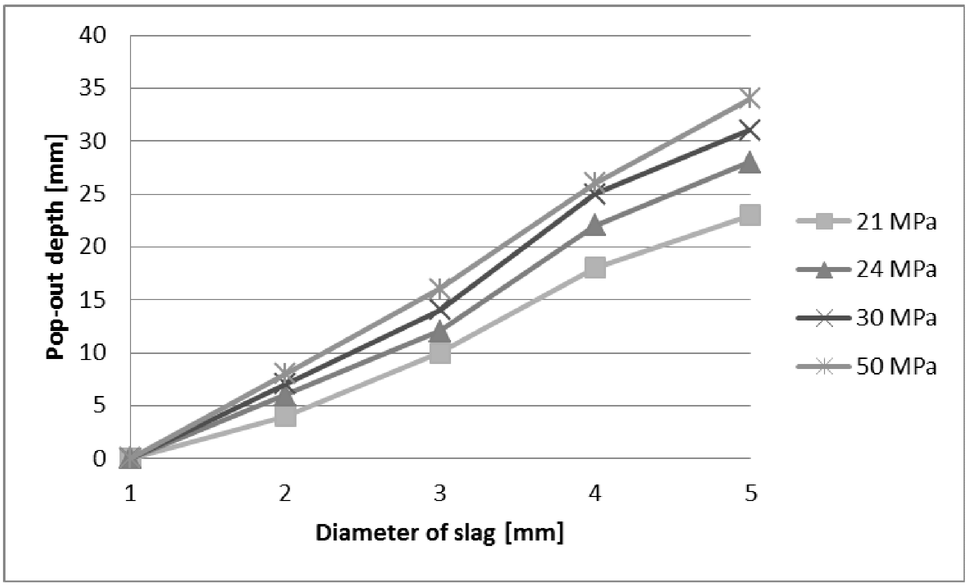

Fig. 2. Concrete cover versus diameter of the slag for different concrete types (from [11])

Other authors [12, 13] made investigations on fine lime particle coming from shrinkage preventing agents or wrong cement manufacturing.

Useful information may be found through the study of other expanding processes [14]: Alkali Aggregate Reaction (AAR) should induce similar stresses inside concrete. A difference is however coming from the easier fulfilling of aggregate cracks by the silica gel which progressively replaces a part of the initial products present along the edge of stone material.

With regard to the very poor information coming from literature reviewing, it clearly appears a lack of knowledge on the behaviour of quick lime aggregates (up to 20mm diameter) when mixed into concrete. A risk evaluation analysis is needed: it will be based on an experimental program and modelling that will help for understanding free lime behaviour in confined situation.

2. Stresses calculation and modelling: theoretical background

2.1. Simplified approach

As a first simplified preliminary approach, it is considered that the swelling pressure is unable to induce cracking in the concrete as a nodule of lime can merely be considered as an air bubble, whose effect is increasing the porosity and, consequently, decreasing the compressive strength of concrete. Bolomey and Feret theories can be used to quantify this phenomenon [15].

Based on the equation p (aggregates) + s (sand) + c (cement) + w (water) + v (voids) = 1, which expresses the sum of the volume fractions for 1 m³ of concrete, we have, with $\lambda = (c/(c + w + v))$, the Feret formula which expresses the relationship between the compressive strength of concrete and the voids (v):

$$f_{c,cube} = K_0\,\lambda^2 = K_0\left[\frac{c}{c+w+v}\right]^2 \quad \text{with } K_0 = K\,.\,R_c \tag{1}$$

where $f_{c,cube}$ is the compressive strength (MPa), K is a granular coefficient and R_c = the compressive strength of cement measured on standardized mortar (EN 196-1),

This clearly indicates that the compressive strength decreases when the w/c ratio increases. If we express this equation as a function of W and C (mass ratio) for a cement relative density of 3.15, the expression can be written:

$$f_{c,cube} = K_0 . \frac{1}{\left(1+3.15\dfrac{W}{C\,(+V)}\right)^2} \tag{2}$$

It is experimentally observed that K is about 4.9 for ordinary concrete [16]. Bolomey formula also suggests a linear relationship between the compressive strength and the ratio C/W.

$$f_{c,cube} = k\left(\frac{C}{W} - h_1\right)$$

where k (26 – 36) and h_1 (0.45 to 0.87) depend on the quality of the cement, the age of the concrete, the shape and dimensions of the test pieces, the curing conditions and the sieving curve of aggregates and sand.

The volume occupied by the nodules can be considered as an additional volume of water in the sense of increasing W/C ratio; that will partially produce an additional volume of air after curing and evaporation. If we consider for example a W/C = 0.5 and a bulk density of lime 1.56 [3], the volume occupied by the nodules, for a percentage of 0.3% of the mass of aggregates into concrete (1300 kg/m^3 of concrete), would be: 0.003 x 1300/1560 = 0.0025 m^3 = 2.5 litres. This means that we can consider a fictitious increase of the amount of water for a 350 kg concrete cement of about 2.5 litres, which means a total of 175 + 2.5 = 177.5 litres. The W/C ratio increases thus from 0.50 to 0.507. Feret formula allows estimating the resulting loss of strength [16]:

$$\frac{1}{(1+3{,}15x0{,}50)^2} / \frac{1}{(1+3{,}15x0{,}51)^2} = 1.017$$

This corresponds to a loss of strength of about 1.7%.

This evaluation clearly shows that the influence of nodules inside the concrete has a very marginal impact on the major structural characteristic of concrete: compressive strength is only lightly affected by a reasonable level of pollution by lime nodules.

However, if these nodules are close to the surface, they are likely to induce pop-out and cracking, which is detrimental for concrete structure durability [17]. Only few data are available on this subject in the literature [10, 12, 18] and mainly deals with the effect of the nodules of lime in steel slag, most often used as aggregates for making concrete blocks [11].

These slags contain mostly dead-burned lime nodules, much slower to react because more compact than the type of lime considered here.

Specific theoretical developments have thus been carried out to assess the risk of such phenomena. Cracking and the emergence of a burst are indeed conditioned by a number of factors related to the materials:

- the depth of the nodule,
- the diameter of the nodule,
- the concentration of nodules,
- the conditions of confinement of the nodule of lime (rate of expansion, swelling pressure),
- tensile strength of the concrete,
- modulus of rigidity of lime (and hydrated lime) and concrete.

For this purpose, simple theoretical models are proposed. These models are based on the mechanics of materials and on the theory of elasticity. The study also assesses the sensitivity of the mechanical effects with respect to the various relevant physical parameters. Two configurations are studied. The first one considers a nodule embedded within the concrete mass: the objectives are in this case to estimate the influence zone of the nodule and the possible risks of interaction between neighbouring nodules, as well as the risk of crushing or cracking of the concrete in the vicinity of the nodule. The second situation is considering a nodule located near the free surface of the concrete, with the main objective of evaluating the risk of occurrence of a pop-out phenomenon.

2.2. Modelling of expansive nodule inside a rigid medium

2.2.1. Behaviour of a nodule embedded within concrete

Model 1 used in this situation considers a spherical nodule in perfect contact with an environment encompassing infinite dimensions. Both media are assumed to exhibit an elastic behaviour. Although both materials are known to be largely inelastic, this model is however appropriate for low level of stresses – and in particular to estimate the initiation of cracking – and can also provide a good understanding of the physical phenomena with a limited computational effort.

Model 1 (Fig. 3) is based on the assumption that the swelling of the nodule is partially prevented by pressure developing at the interface between concrete and lime and confining the nodule. This pressure depends on the mechanical properties (elastic modulus and Poisson's ratio) of the two materials, as well as on the amplitude of the swelling as it would be observed if the nodule was perfectly free to expand upon hydration. Assuming a spherical symmetry of the problem and a perfect compatibility of the displacements at the interface between lime nodule and concrete matrix, the pressure can be calculated using equation 3, on the base of the relations proposed in [19] for spherical containers under internal or external uniform pressure:

$$p = \frac{\frac{\Delta R}{R}}{C_L + C_C} \qquad (3)$$

with

$$C_L = \frac{1 - 2\nu_L}{E_L} \qquad (4)$$

and

$$C_C = \frac{1 - 2\nu_C}{E_C} \qquad (5)$$

where E_L and E_C are the elastic modulus of hydrated lime and concrete, respectively, ν_L and ν_C are the Poisson's ratio of hydrated lime and concrete, respectively, R is the initial radius of the nodule and ΔR the variation of the radius of the nodule due to hydration process.

ΔR/R ratio can be directly related to volume variation by means of equation 6:

$$\frac{\Delta R}{R} = \sqrt[3]{\frac{V_{final}}{V_{initial}}} - 1 \quad (6)$$

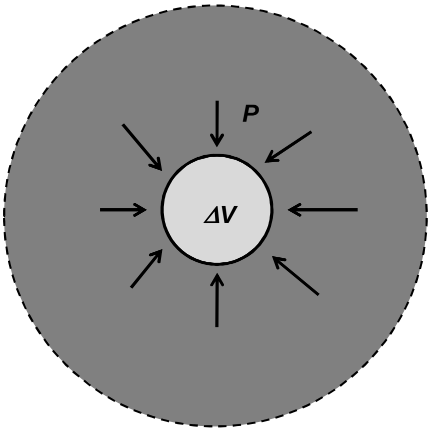

Fig. 3. General principle of the model of embedded nodule

If a perfect contact is assumed with a contact pressure fully developed, it is possible to calculate the stress distribution in the surrounding medium from the elasticity theory, as proposed in [19]. It is needed to distinguish compressive stresses σ_r, acting in radial direction, and tensile stresses σ_t, oriented in the circumferential direction. They are given by equations 7 and 8, respectively:

$$\sigma_r = -p\frac{(D/2)^3}{\left(\frac{D}{2}+z\right)^3} \quad (7)$$

and

$$\sigma_t = \frac{p}{2}\frac{(D/2)^3}{\left(\frac{D}{2}+z\right)^3} \quad (8)$$

In these equations, the stresses are positive in tension and negative in compression. Furthermore, D is the diameter of the inclusion and z is the distance from the interface concrete/inclusion to the considered point inside the concrete.

These stresses can then be compared to the compressive and tensile strength of the concrete in order to assess the risk of a local crushing around the nodule or of occurrence of radial cracks associated with circumferential tension in the vicinity of the nodule. On the other hand, the model allows estimating the area of concrete mechanically disturbed by the presence of a swelling nodule.

2.2.2. Effect of a nodule in the vicinity of the concrete surface

A second model (Fig. 4) is used to assess the risk of local bursting of concrete (*pop-out*). It is now assumed that the swelling pressure is no more balanced by a stress distribution with spherical symmetry, but rather by a tensile stress distribution varying linearly from the inclusion towards the surface and distributed on a truncated cone.

Based on this failure pattern, one can evaluate the maximum tensile stress acting at the base of the truncated cone with the following equation:

$$\sigma_t = \frac{pR^2}{\left[\frac{(R+e)^2}{3tg^2\beta} + \frac{R(R+e)}{tg\beta}\right]} \quad (9)$$

where R is the radius of the nodule, p is the pressure induced at the interface between nodule and concrete, e is the thickness of concrete covering and β is the angle of the ejection cone with respect to the concrete surface. Equation 9 simply translates the fact that the resultant of swelling pressure acting on the bottom part of the nodule is directly balanced by the vertical resultant of tensile stresses acting at the surface of the ejection cone and that the *pop-out* effect is initiated when the local tension stresses exceed the tension resistance of the concrete matrix.

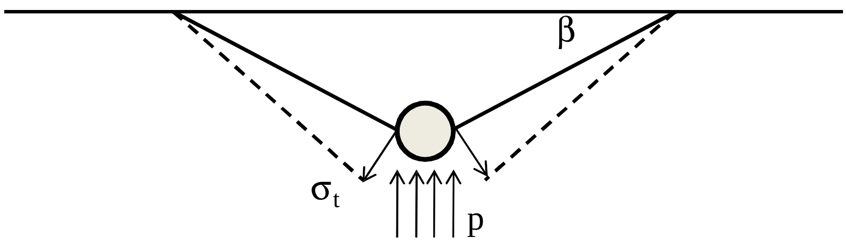

Fig. 4. Principle of concrete rupture due to near-to-surface swelling nodule

Based on the evaluation of the swelling pressure obtained from model 1, tensile stress can be calculated from model 2 and compared to the tensile strength of concrete to assess the risk of pop-out.

3. Description of the experimental program

The objectives of the experimental investigations and analyses were:

- to observe the behaviour of a lime nodule embedded into concrete,
- to quantify expansion rate of lime,
- to characterize the quality of hydrated lime (densification process),
- to select data for calculation modelling (expansion and compressibility modulus of free lime).

3.1. Selection and preparation of materials

Free lime (from 80 to 120 mm limestone blocks) is representative of a production process with a classical reactivity (T_{60} = 2 min17 s) and purity; density is equal to 1.44 g/cm^3. Samples (Φ = 18.5 mm and H = 15 to 20 mm) are cored in the lump lime. Concrete blocks of (190x190x85) mm³ have been firstly used to simulate confining effect. They provide a compressive strength of 15 N/mm^2 and a density of 2.2 g/cm^3. This type of porous concrete has been selected in order to favour water transmission and lime reaction.

3.2. Confining operations

A cylindrical opening of 19 mm diameter (Fig. 5a) and 25 mm deep (Fig. 5b) is cored in the blocks by means of a drill. To study the impact of the situation of the nodule of lime from the concrete surface, the holes are made at different distances from the edge of the concrete block (Fig. 5c). To ensure the best confinement possible, finishing cylindrical orifices are performed with quick-setting cement to fill the cone left by the bit, to smooth the cylinder walls and to repair the damaged edge of the whole drilling. However, despite these precautions, confinement is not perfect: the top surface of the block is not perfectly flat and a minimum clearance is required to introduce the carrot in his hole (Fig.5d).

(a)

(b)

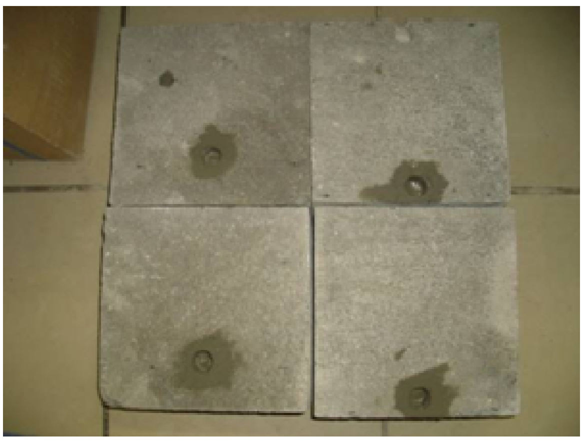

(c) (d)

Fig. 5. Preparation of the concrete blocks.

The confinement of the concrete block is then ensured by steel plates and clamps. A plastic sheet is inserted under the steel plate for preventing any reaction between lime and steel (Fig. 6). The assembly is then immersed in water and the water level is adjusted under the top edge of the block (Fig. 7).

Fig. 6. Confinement of the free lime nodule inside the concrete.

Fig. 7. Immersion of the concrete block into water.

A reference test is made in order to check the time needed for a complete hydration of a free lime cylinder: it was measured that 67 hours storage into water allowed a full hydration of the sample by means of water transfer through the porosity of the sample.

The blocks are then cut with a diamond saw (dry) at the right and the edge of the nodule, in order to observe possible internal cracks. Hydrated lime cores are then recovered, measured, weighed and analyzed on the base of the loss on ignition at 100 °C (moisture measurement) and 600 °C (measuring the rate of hydration).

3.3. X Ray Diffraction and Microscopical analysis

X Ray Diffraction anlyses have been carried out in order to determine the mineralogy of the crystals and the nature of the hydrated products.

Samples observed with Environmental Scanning Electron Microscope (ESEM) are similar to the one used for XRD investigations. The samples are glued on metal pads using a conductive adhesive. The specimens are thus metallized with Pt before being introduced into the vacuum chamber of a scanning electron microscope ESEM. The electron beam gives a view of topography and shape of hydrated lime. EDAX (Philips) system, coupled with ESEM, allows the detection of elements identified on a spectrum according to their energy dispersion.

These analyses allow obtaining a good identification of different forms of calcium hydroxide crystals under confinement.

4. Results and discussions

4.1. Stress calculation and modelling hypothesis

In order to feed the proposed models, data needed are:

- Elastic modulus of hydrated lime and concrete,
- Poisson's ratio of hydrated lime and concrete,
- Variation of volume of nodule during hydration.

The elastic modulus and Poisson's ratio of lime are estimated from [20]: the value used for the elastic modulus of 100 MPa and Poisson's ratio is 0.25. Results obtained from the experimental program running in parallel with the present theoretical study indicate similar values (chapter 4). The module of the concrete is of the order of 30 GPa and its Poisson's ratio is considered equal to 0.2. It will be shown later on that the results are quite insensitive to these latter values.

The swelling rate is more difficult to estimate. In fact, if the volume variation of the lime during hydration can reach values as high as 200%, these values are only relevant in the absence of any confinement. The tests carried out in the framework of the present study show indeed that the volume variation significantly depends on the stiffness and strength of the confining medium. The results presented in chapter 4 and other tests on lightweight concrete blocks show that, if one measures the change in diameter of cylindrical samples in the direction of confinement (i.e. in the radial direction) for samples with a diameter which is adjusted to the initial hole made in the confining medium, and which therefore are in contact with this medium from the start of the hydration reaction, the average value of $\Delta R/R$ is:

- 22% for confinement in cellular concrete block of 2 MPa compression characteristic strength,
- 16% for confinement in cellular concrete block of 4 MPa compression characteristic strength,
- 7% for confinement in a heavy concrete block of 15 MPa compression characteristic strength.

These values correspond to respective volume variations $\Delta V/V$ of 49, 34 and 15%, respectively.

This observation is explained by the fact that, when the confining pressure reaches a sufficient level, it forces the hydration reaction to occur towards the inside of the lime sample. This reaction proceeds thus at constant volume and pressure, but results in a more dense hydrated material. It is therefore expected that its elastic modulus be higher than the reference value of 100 MPa.

Equations 7, 8 and 9 cannot be directly applied in the purpose of comparison with the case of cylindrical test samples: the above equations indeed assume a spherical inclusion. The transition to the cylindrical case, however, can be done quite simply by changing the coefficients C_b and C_{ch}:

$$C_L = \frac{(1-2\nu_L)(1+\nu_L)}{E_L} \tag{10}$$

and

$$C_C = \frac{1+\nu_C}{E_C} \tag{11}$$

Taking into account this adaptation, it is possible to evaluate contact pressure developed for the different test conditions (Table 2).

Table 2

Evaluation of the contact pressure vs lime and concrete properties

	E_C (MPa)	**$\Delta R/R_{mean}$ (%)**	**$\Delta R/R_{max}$ (%)**	**P_{mean} (MPa)**	**P_{max} (MPa)**
Cellular concrete block C2	2,000	22	24	32	35
Cellular concrete block C4	4,000	16	19	24	29
Concrete	15,000	7	12	11	19

One might conclude from values in table 2 that the pressure required to confine the reaction varies with the material. It must however be noted that the model assumes an elastic behaviour of the confining material whatever the value of the pressure, while an evaluation of the stresses developed in the confining medium for the cellular concrete block case (i.e. $\sigma_{c,max} = p$ and $\sigma_{t,max} = p/2$) concludes that they exceed by far the resistance of the blocks. Calculations show that, for a sample of 18 mm diameter, the resistance is actually exceeded on a thickness approximately equal to the diameter of the sample. It can therefore be estimated that the effective stiffness of the zone of the confining medium directly surrounding the inclusion is reduced with respect to its reference undamaged value, thereby increasing the value of the coefficient C_C and reducing consequently the pressure so as to reach a balanced situation between effective stiffness and pressure. A refined modelling of this phenomenon would however require advanced tools that are considered out of the scope of the present study. One must also note that cracks were indeed observed in the zone surrounding the inclusion for some of the cellular concrete blocks used for confinement tests, which is in accordance with the above conclusions. On the other hand, for an ordinary concrete containment, the calculated level of pressure is such that the stress remains at a level below the resistance of the material. The model reproduces thus correctly the experimental trends.

The range of parameters considered for the upcoming parameter studies is defined by:

- E_C: 7000, 15000 and 30000 MPa, which corresponds to concrete confinement ranging from poor characteristics to ordinary concrete;
- E_L: 100 to 200 MPa, ranging from a normal value to a value doubled to take into account densification of lime during hydration. Experimental tests shows actually that, for the samples corresponding to hydration in heavy concrete blocks, and thus with the highest densification rate, the value of the measured elastic modulus is about 150 MPa;
- ν_L and ν_C equal to 0.25 and 0.20 (values from the technical literature);
- Change in volume of the spherical inclusion varying from 10 to 50%, which corresponds to changes in radius of 3 to 15%. This range roughly sweeps the radius

variation observed during tests on hydration inside the heavy concrete blocks (observed values varying between 3 and 12%).

Finally, it must be stated that, as illustrated in Fig. 8, the pressure level provided by the model for a given volume variation ($P_{fin,model}$) is obviously an upper bound of the actual value ($P_{fin,actual}$) due to the following reasons:

- The model assumes that the inclusion and the confining materials are in perfect contact and exhibit a spherical symmetry, while they actually very often show significant shape irregularities. In order to provide order of magnitudes, it is relevant to note that, for same volume variation and initial diameter, the pressure calculated for a cylindrical inclusion is 25% less than the one calculated for a spherical inclusion (i.e. the slope α of the real "pressure *vs* volume" curve is lower than the one given by Eq. 3 and 6);
- The model assumes that the contact is established from the beginning of swelling. In reality, it can be assumed that a part ΔV_0 of the measured volume variation is corresponding to the filling of the voids between the inclusion and the matrix; the real pressure should therefore be associated with only a fraction of the volume change;
- The model assumes that the elastic modulus of lime is constant throughout the swelling phase, whereas it is in fact a phenomenon whose parameters vary with time. The mechanical characteristics α_{ini} of hydrated lime at the initiation of the swelling are corresponding to an unconfined environment and progressively evolve to those (α_{fin}) of hydrated lime properties in confined environment. The model conservatively considers the stiffer situation (α_{fin}) throughout the entire swelling process.

The level of conservatism of the chosen modelling assumptions is however quite impossible to quantify.

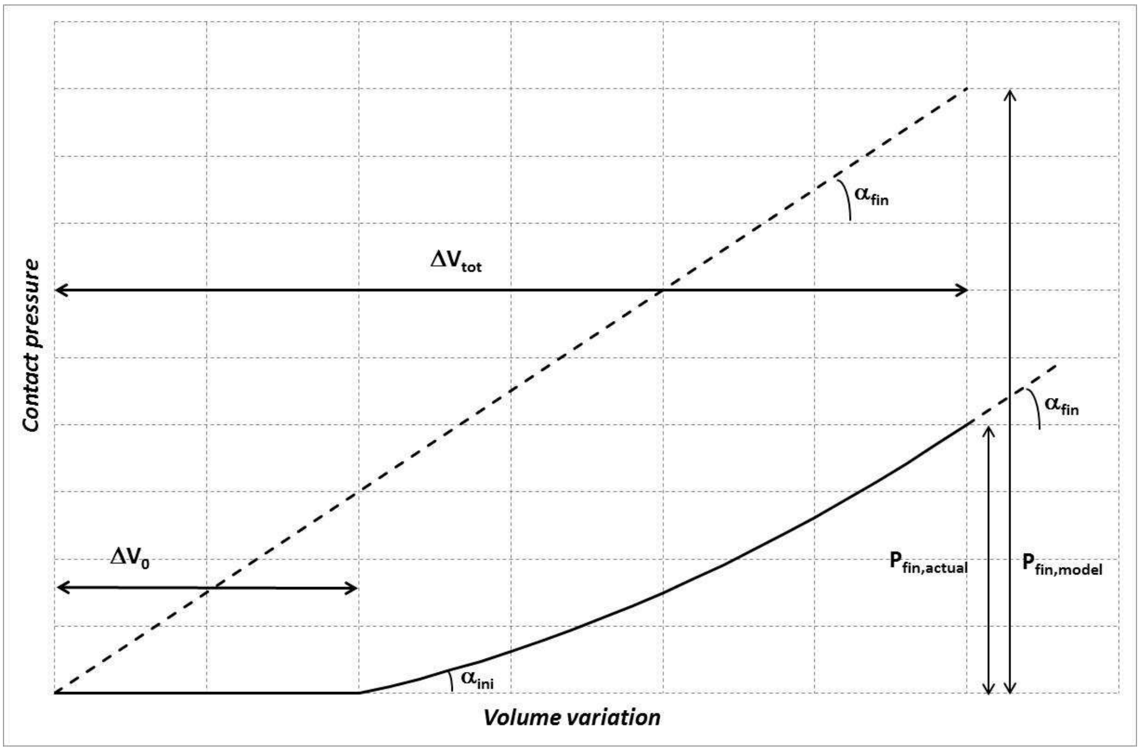

Fig. 8. Comparison of the actual and assumed pressure/volume relationship

4.2. Model exploitation and parametric study

4.2.1. Evaluation of the contact pressure

Results of the calculation of the contact pressure are presented on Table 3. It is showed that pressure is roughly independent from the quality of concrete. However, results are clearly influenced by the rigidity of the lime and the variation of the volume: estimated pressure ranges from 6 to 57 MPa (this latter value is clearly unrealistic but defines an absolute upper bound that would never be overtaken even for the worst conditions). It has also to be mentioned that a possible variation of the Poisson's ratio of the lime could induce significant variation of the pressure: e.g. for an elastic modulus equal to 100 MPa, a variation of volume corresponding to 30% and Poisson's ratio equal to 0.2, 0.25 and 0.3, resulting pressure is equal to 15, 18 and 23 MPa respectively.

For the reasonable average values of the parameters (E_L = 150 MPa and volume variation of 20%), pressure is up to 19 MPa, which is however a clearly conservative estimate of the real pressure, as illustrated on Fig. 8.

Table 3

Evaluation of the contact pressure *vs* E modulus of lime (E_L) and concrete (E_C) and volume (radius) variation of lime

E_L (MPa)	**ΔV/V (%)**	**ΔR/R (%)**	**p [E_C=7000] (MPa)**	**p [E_C=15000] (MPa)**	**p [E_C=30000] (MPa)**
	10	3	6	6	6
	20	6	12	12	12
100	30	9	18	18	18
	40	12	23	24	24
	50	14	28	29	29
	10	3	9	10	10
	20	6	18	19	19
150	30	9	27	27	27
	40	12	35	35	35
	50	14	42	43	43
	10	3	12	13	13
	20	6	24	25	25
200	30	9	35	36	36
	40	12	46	47	47
	50	14	56	57	57

4.2.2. Stress distribution

Compressive and tensile stress distributions are given in Figs. 9 and 10 for several values of pressures and nodule diameters. Curves are corresponding to 3 levels of pressure taken from Table 3:

- P_{min} = 6 MPa (pressure calculated on the base of minimalistic hypotheses),
- P_{mean} = 19 MPa (pressure conservatively calculated on the base of most probable hypotheses),
- P_{extr} = 57 MPa (pressure upper bound calculated on the base of extreme hypotheses).

Values of stresses are calculated for 3 lime nodule diameters: 2, 10 and 20 mm, respectively. On Fig. 9 providing tensile stresses, horizontal straight line corresponds to the mean tensile strength of ordinary C25/30 concrete.

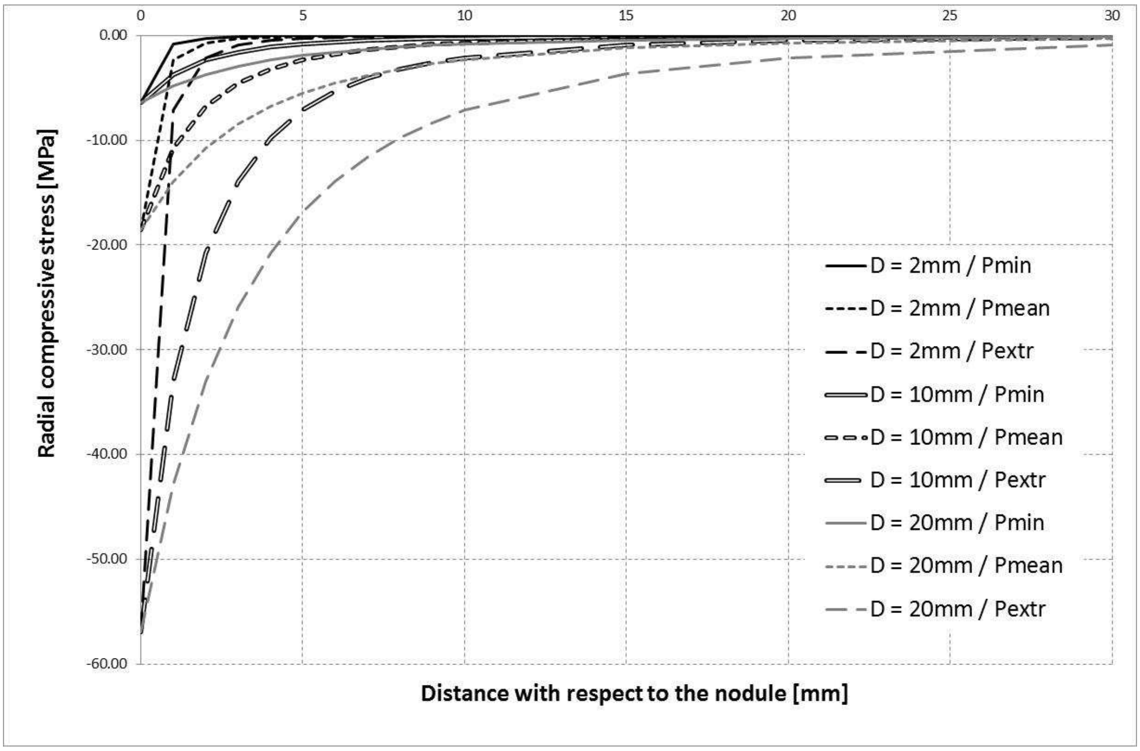

Fig. 9. Evolution of compressive stresses *vs* contact pressure and nodule diameter

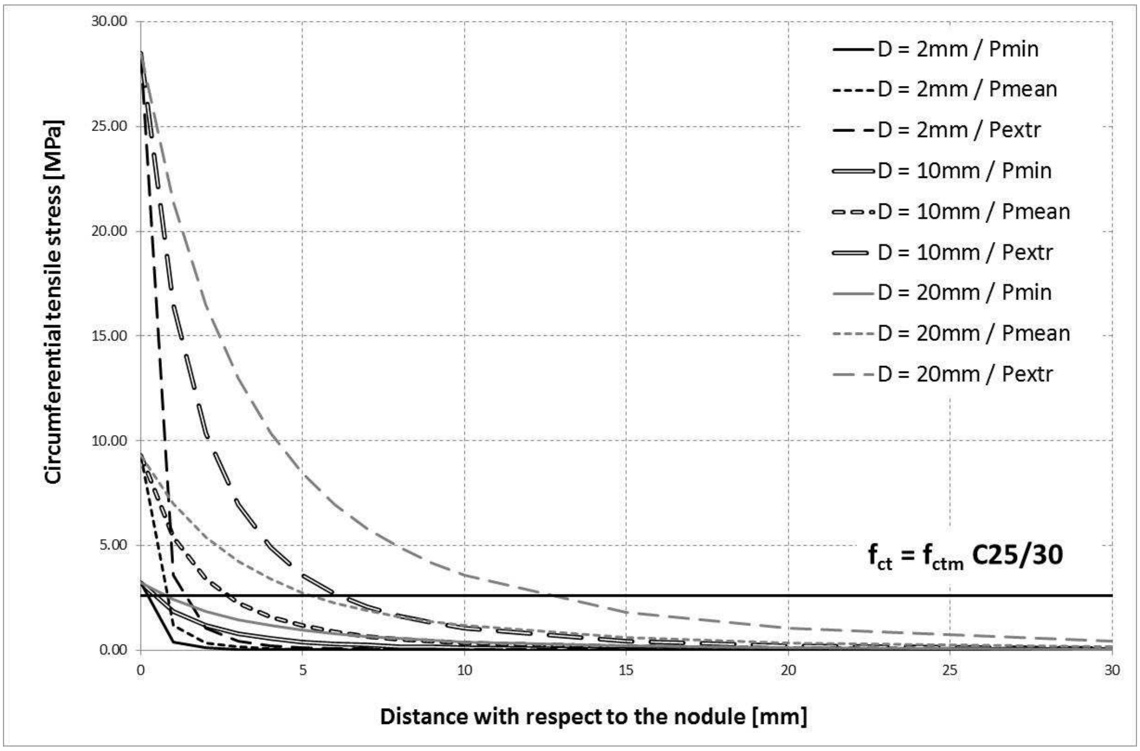

Fig. 10. Evolution of tensile stresses *vs* contact pressure and nodule diameter

The figure related to compressive stresses (Fig. 9) shows that, around a nodule which is assumed to be perfectly smooth and spherical, the stress level is equal to the pressure. For extreme conditions, this level is likely to exceed the level of resistance of ordinary concrete. However, for average conditions, this level remains acceptable. The curves also clearly show that the stress level rapidly decreases with the distance from the nodule. Consequently, at a distance equal to two times the diameter, the stress level is only about 1% of the pressure and goes down to less than 0.1% at a distance corresponding to 5 times the diameter. It can therefore be concluded that:

- Local crushing of the concrete near the nodule is normally not to be feared;
- The area of influence of a nodule is of the order of 2 to 3 times the diameter (measured from the centre of the nodule). Assuming that the minimum distances between nodules are in the order of 100 mm, the areas potentially impacted by the presence of nodules are unlikely to interfere.

Fig. 10 shows that, except for the minimum conditions, there exists a region around the nodule where tensile forces are potentially present and thus likely to initiate micro-cracking. No significant cracking has however been observed in tests performed in the laboratory for lime hydration in heavy concrete blocks (chapter 4). Table 4 gives the thickness of the potentially cracked area corresponding to a module of lime E = 150 MPa for different values of the volume change and of the tensile strength of the concrete (corresponding to percentiles of 5, 50 and 95, respectively, for standard concrete C25/30).

Table 4

Thickness of the potentially cracked zone around nodule of D diameter *vs* tensile strength

ΔV/V (%)	**$fct = fct_{C25/30,5\%} = 1.8$ (MPa)**	**$fct = fct_{C25/30,50\%} = 2.6$ (MPa)**	**$fct = fct_{C25/30,95\%} = 3.3$ (MPa)**
10	0.19 D	0.11 D	0.07 D
20	0.36 D	0.26 D	0.21 D
30	0.48 D	0.37 D	0.30 D
40	0.57 D	0.45 D	0.37 D
50	0.64 D	0.51 D	0.43 D

One must be reminded that the values of radial swelling measured in the laboratory (chapter 4) are of the order of 7 % (so corresponding to a volume variation ΔV/V about 15 %). However, in the worst case (ΔV/V = 50 %) and for a very low concrete tensile strength (1.8 MPa), the thickness of the cracked area is potentially of the order of 64% of the diameter. Under these conditions, if these cracked zones are fully assimilated to non-resistant inclusions with a diameter equivalent to 2.28 times the diameter of the nodule (i.e. 1D + 2 x 0,64D), the calculation of the effect of voids on the compressive strength of concrete according to section 1 of the present paper shows that, even in the case of cracking around all the nodules included in the concrete (for a reasonable concentration of such lime nodules), the overall strength of the concrete would hardly be affected.

4.2.3. Pop-out risk estimation

Figures 11, 12 and 13 represent the results obtained by using the equation 9 to estimate the risk of pop-out. These figures actually represent the minimum thickness of the concrete cover beyond which the theoretical model predicts no occurrence of pop-out. This thickness is plotted as a function of the diameter of the inclusion for different values of the tensile strength of concrete and of the swelling pressure of the nodule. The ejection angle is chosen equal to 30° in accordance with common observations made on site. For facilitating the reading of the charts, a light grey dash line outlines the situation where concrete thickness equals the diameter of the nodule.

The following observations can be drawn from the analysis of these figures:

- For the minimal assumptions (low elastic modulus of the lime and low inflation rate - Fig. 11), the risk of pop-out is almost negligible. The model predicts occurrence of pop-out only for very low quality of concrete (fct equal to 1.8 MPa). For higher values of fct, the estimated risk of pop-out is zero whatever the cover thickness, as shown on Fig. 11 by perfectly horizontal superimposed lines corresponding to fct equal to 2.6, 3.3 and 5.0 MPa. Even in the worst case, a cover thickness less than 10% of the diameter appears sufficient to prevent pop-out;
- For the most realistic though conservative assumptions (intermediate modulus of the lime and swelling ratio of 20% in volume - Fig. 12), the risk of pop-out is more important. For a tensile strength corresponding to ordinary concrete (2.6 MPa), the

risk of pop-out occurs if the thickness of the covering is of the order of half of the diameter (50 %) of the inclusion. This is to be compared with hydration tests on heavy concrete blocks (inclusions approximately 20 mm diameter) for which pop-outs have been observed only for cover thicknesses of 10 and 5mm (i.e. 50 and 25% of the diameter). Modelling and observations seem to provide convergent results, confirming thus the assumptions made on the different parameters entering in the modelling process;

- For extreme cases (Fig. 13), the model predicts ejection of pop-outs for thicknesses of less than 1 to 2 times the diameter, according to tensile strength of the concrete.

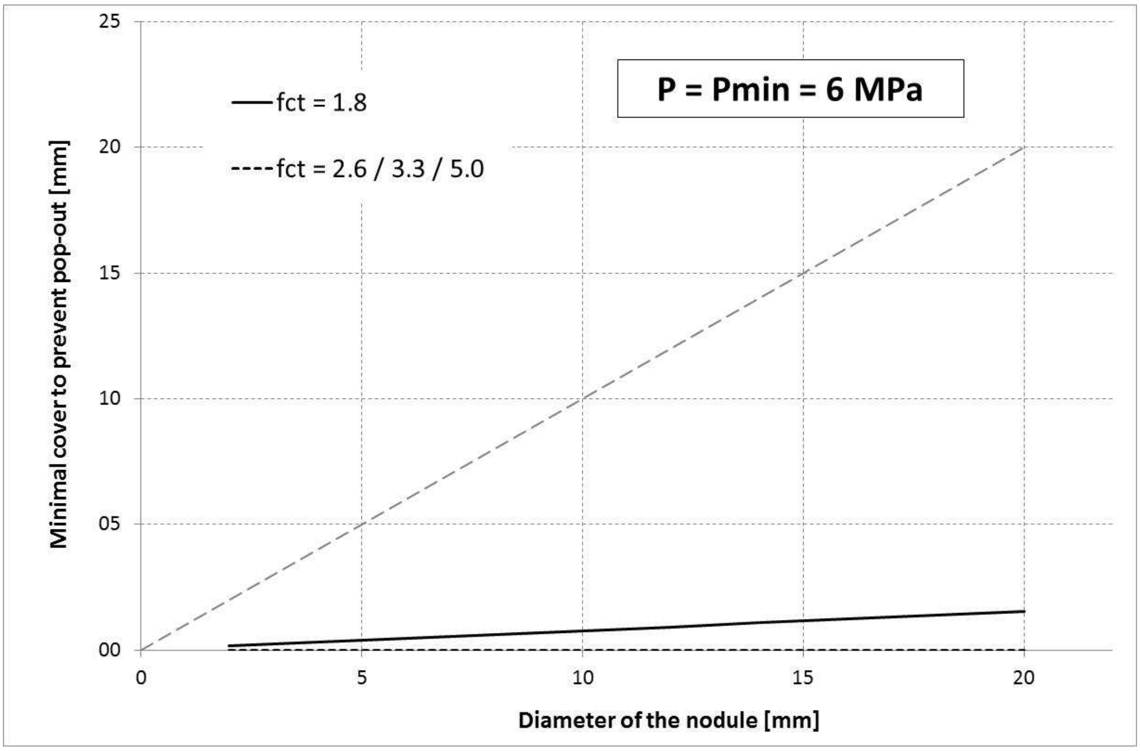

Fig. 11. Evolution of the minimal thickness of concrete cover *vs* nodule diameter (minimum pressure).

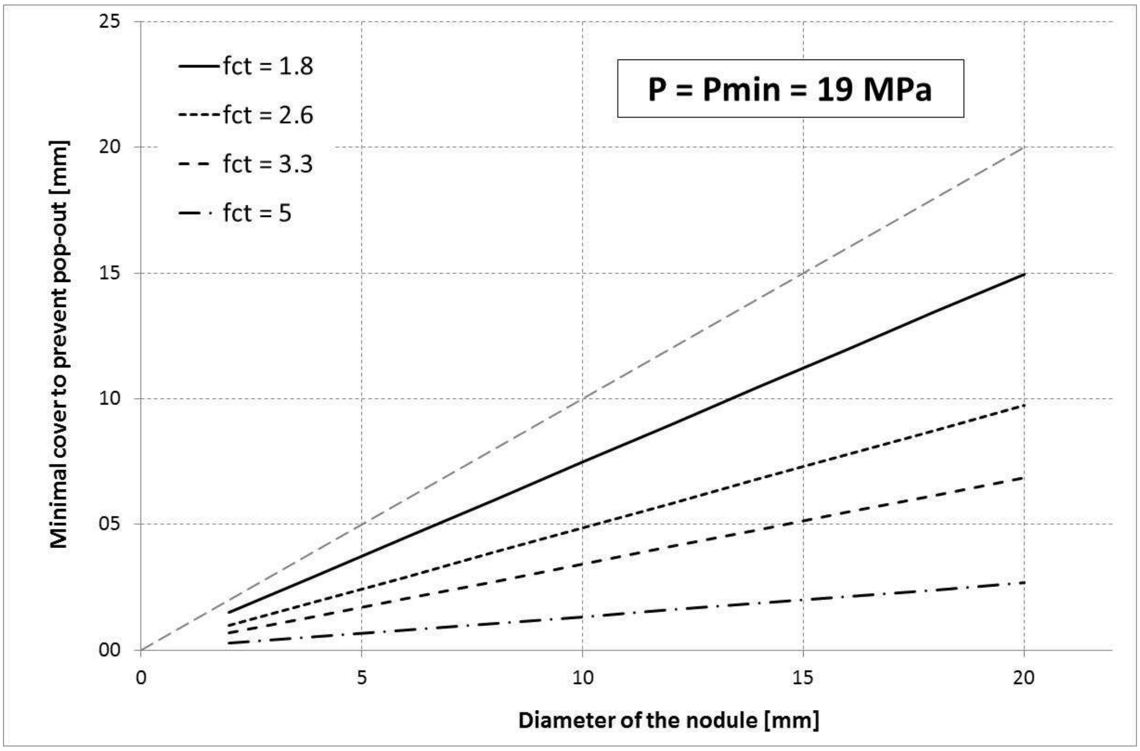

Fig. 12. Evolution of the minimal thickness of concrete cover *vs* nodule diameter (mean pressure).

466

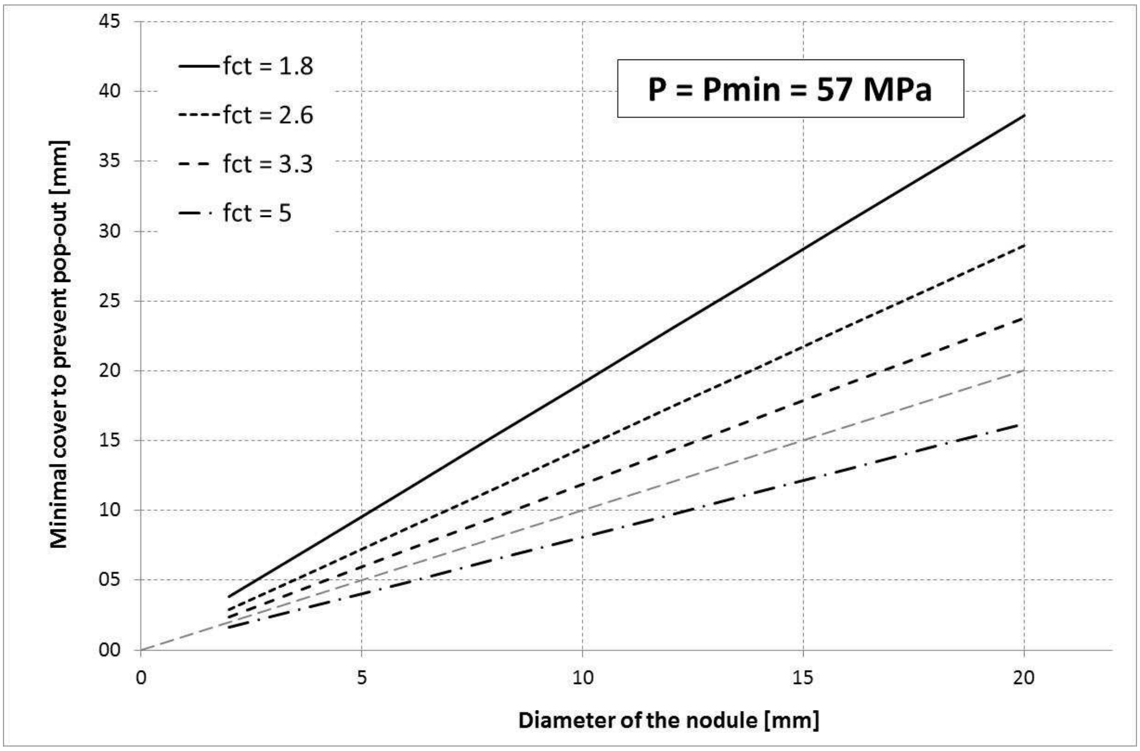

Fig. 13. Evolution of the minimal thickness of concrete cover vs nodule diameter (maximum

pressure)

4.3. Confined free lime hydration results

4.3.1. Results of the tests

Eighteen trials were conducted, including 16 in the form of maximum confinement (tests 1 to 16) and two under restricted confinement (tests 17 and 18), leaving more place for the hydrate to crystallize: the confinement is in fact restricted if the carrot of lime is of a size smaller than the hole in the concrete. In this case, the metal plate is not completely in contact with the concrete surface and allows some expansion of the lime. Several distances D from the edge of the concrete substrate were tested: 4.5 to 0.25 times the initial diameter d of the core of lime, respectively D/d in Table 6).

After testing conditions 8, 9, 13 and 17, respectively, loss of ignition at 600°C was measured in order to evaluate the rate of hydration of the lime (Table 5).

Table 5

Hydrated lime content of the samples.

Test	Loss of ignition at 600°C [%]	$Ca(OH)_2$ content [%]
8	24.2	99.6
9	23.9	98.1
12	23.6	96.9
17	23.7	97.4

A minimum value of 97 % of $Ca(OH)_2$ is measured. If we consider that initial lime is not totally pure – it means less than 100% CaO due to unburn limestone - , we may conclude that all the free lime has been hydrated.

4.3.2. Internal cracking of the concrete blocks and pop-outs

No cracking has been observed for all the concrete blocks tested (Fig. 14 a to e). Even for free lime nodules very close to the concrete surface (0.5 times free lime nodule diameter), no cracking appeared inside the block.

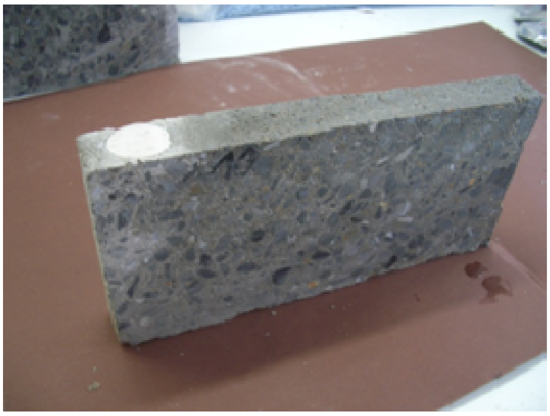

(a) Free lime nodule at 10 mm depth

(b) Free lime nodule at 20 mm depth

(c) Free lime nodule at 40 mm depth

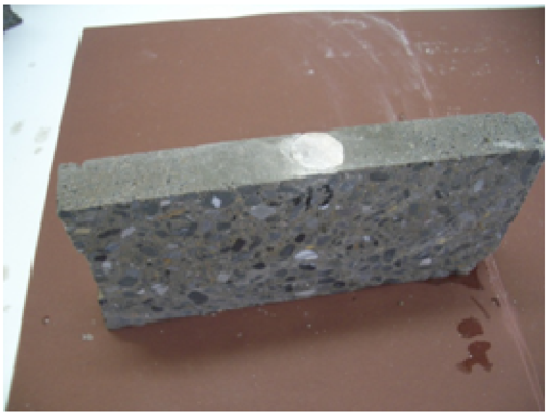

(d) Free lime nodule at 90 mm depth

(e) Free lime nodule at 5 mm depth : pop out but no internal crack

Fig. 14. Sections of concrete blocks and free lime nodules.

Pop-outs were observed only for specimens (Fig. 15a and b) corresponding to depths:

- 0.25 times free lime nodule diameter (2 by 3 of the specimens) and
- 0.5 times free lime nodule diameter (1 by 3 of the specimens).

When depth was higher than 1 times the free lime nodule diameter, no pop-out was observed.

(a) (b)

Fig. 15. Free lime nodule at 5 mm depth (a) and 10 mm depth (b).

4.3.3. Analysis of densification phenomenon and nodule expansion

As described in §3.2, the blocks are cut with a diamond saw (dry) at the right and the edge of the nodule and hydrated lime cores are then recovered, measured and weighed. As a reminder, in unconfined conditions, when quicklime CaO (bulk density about 1.5 g/cm^3) is transformed into $Ca(OH)_2$ hydrate, it is in the shape of a powder of low density (about 0.5 g/cm^3). The measurements show (Table 6), in confined situation, a densification process of the hydrate which offers a density much higher than in unconfined case. During these tests, the hydrates obtained in confined environment showed a density varying from 1.4 to 1.7 g/cm^3, with average value of 1.55 g/cm^3 (Table 6).

Table 6

Measurements of confined lime cylinders in concrete blocks (D is the distance between the nodule and the surface and d is the diameter of the nodule)

	Test	Initial lime		Observations		Characteristics of hydrate			
		Density (g/cm³)	D/d	Pop-out (Y/N)	Cracking (Y/N)	Density (g/cm³)	Volume expansion (%)	Radial expansion (%)	Longitudinal expansion (%)
Maximal confinement	1	1.38	4.5	N	N	1.39	32	10	8
	2	1.58	4.5	N	N	1.71	22	5	11
	3	1.44	4.5	N	N	1.62	18	7	4
	4	1.44	4.5	N	N	1.67	14	3	6
	5	1.38	4.5	N	N	1.47	24	6	11
	6	1.49	4.5	N	N	1.54	28	8	9
	7	1.47	2	N	N	1.66	17	8	1
	8	1.39	2	N	N	1.50	23	6	8
	9	1.43	1	N	N	1.49	27	8	8
	10	1.40	1	N	N	1.55	20	8	3
	11	1.41	1	N	N	1.52	23	6	9

	12	1.46	0.5	Y	N	unrecovered			
	13	1.50	0.5	N	N	1.50	32	12	5
	14	1.39	0.5	N	N	1.46	25	7	10
	15	1.45	0.25	Y	N	unrecovered			
	16	1.51	0.25	Y	N	unrecovered			
Restricted	17	1.41	2	N	N	1.14	64	24	76
confinement	18	1.50	0.25	N	N	1.31	51	27	73

This densification process logically implies a volume expansion factor much lower than what is generally known when unconfined (300% as calculated from the ratio of 1.5 g/cm^3 for lime divided by 0.5 g/cm^3 for $Ca(OH)_2$ hydrated lime). Expansion factors measured here are in the range from 15 to 30% (23% average). Figure 16 shows the experimental values in the case of a high confined situation (tests 1 to 16, rhomb dots) and in the case of a partial confinement (tests 17 and 18, square dots).

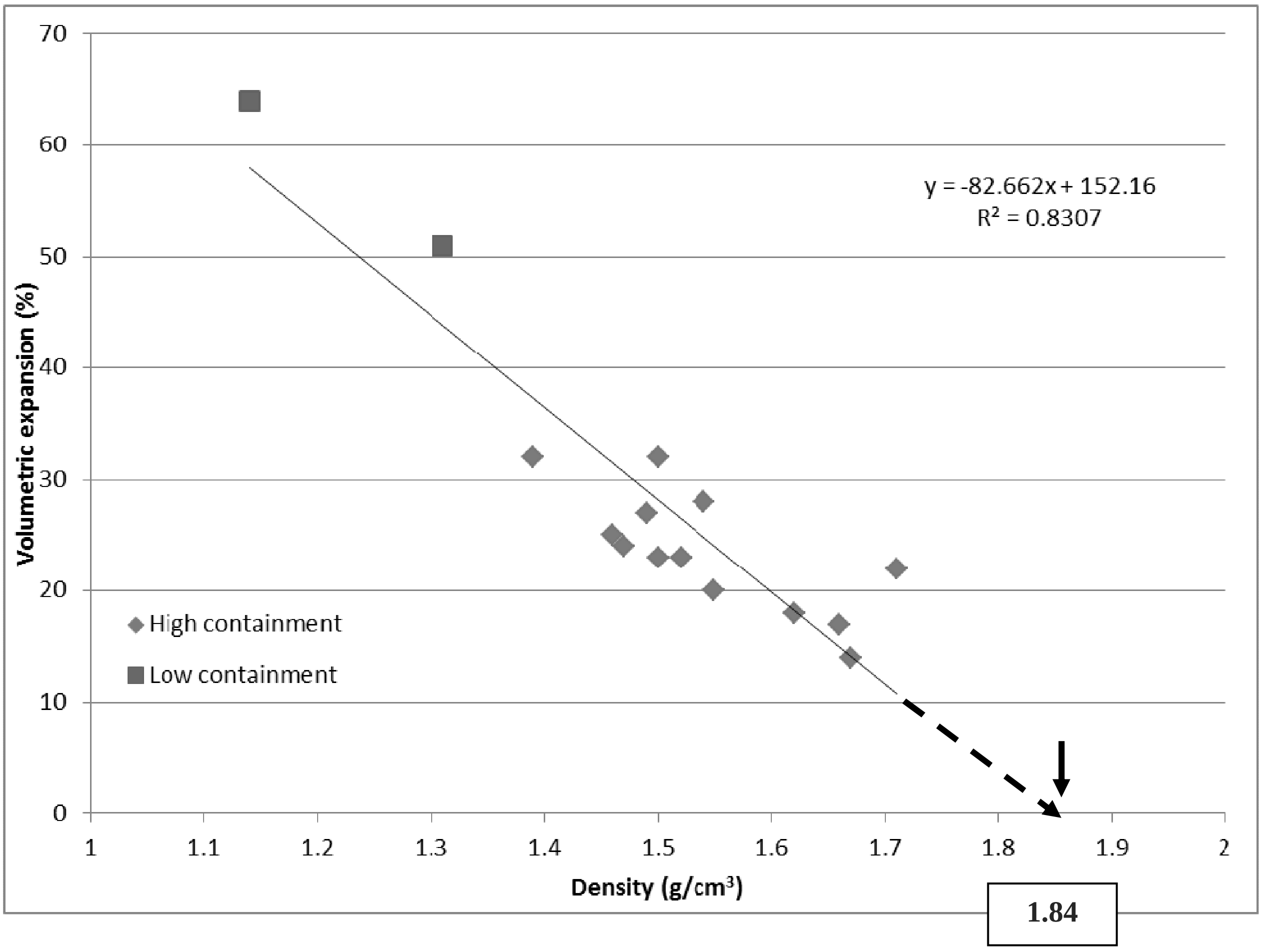

Fig. 16. Evolution of the density of hydrated lime vs volume expansion (confined (tests 1 to 16) and less confined (tests 17 and 18))

The positive expansion that is observed in the case of confined samples (rhumb dots) means that these confinements are not perfect, leaving a free space for expansion. This imprecision is statistically distributed across different samples. These expansions are not related to a deformation of the concrete block. It is possible to estimate the density of the core hydrate in the case of perfect confinement by extrapolating the regression line. This extrapolation (82% correlation) allows to calculate that, in the case of perfect confinement (no volume expansion), the hydrate, formed from lime industrial bulk with a density of 1.5 g/cm^3, will have an equivalent density of 1.84 g/cm^3: this remains less than the absolute density of the hydrate (2.2 g/cm^3).

The tests allow concluding that hydration of quicklime in a confined environment, leads to the production of completely hydrated portlandite nodules with very high densities.

4.3.4. Rigidity modulus

Some values from 100 to 200MPa are given in the literature [19]. Due to the intrinsic variability of the free lime, tests have been performed on cylinder used for testing confinement effect. Samples are prepared exactly in the same conditions than in §3.2: after 67 hours hydration, cylinders are cored from concrete blocks (Ø20mm and H15-20mm). Until testing, specimens are stored into plastic bags in order to avoid carbonation process. Compressive loading is applied at a speed of 5N/s on INSTRON 5585 tensile machine (Table 7).

Table 7

Rigidity modulus and compressive strength of hydrated lime cylinders (MPa).

Specimen reference	Compressive strength [MPa]	Rigidity modulus [MPa]
13 centered*	5.1	150
14 centered**	5.1	164
17 centered	5.4	189
2C20	8.3	168
4C10	3.8	129
5C40	5.3	180
10C10	5.4	144

* small crack at mid-height

** non parallel faces

These indicative measurements confirm literature results and have been used as reference values for modelling (chapter 3).

4.3.5. Hydrated lime analysis

X Ray Diffraction analyses have been carried out in order to determine the mineralogy of the crystals and the nature of the hydrated products. Several samples have been recorded:

- NC1 : not confined sample (100% free volume V_f)
- C110 : Ø10 mm sample confined into concrete hole of ± 20 mm diameter (± 75% V_f)
- C115: Ø15 mm sample confined into concrete hole of ± 20 mm diameter (± 44% V_f)
- C120: Ø20 mm sample confined into concrete hole of ± 20 mm diameter (± 0% V_f)

On diffractograms (Fig. 17), it appears that all the samples are of Portlandite type $Ca(OH)_2$. Calcite can be present in very few quantities, due to carbonation.

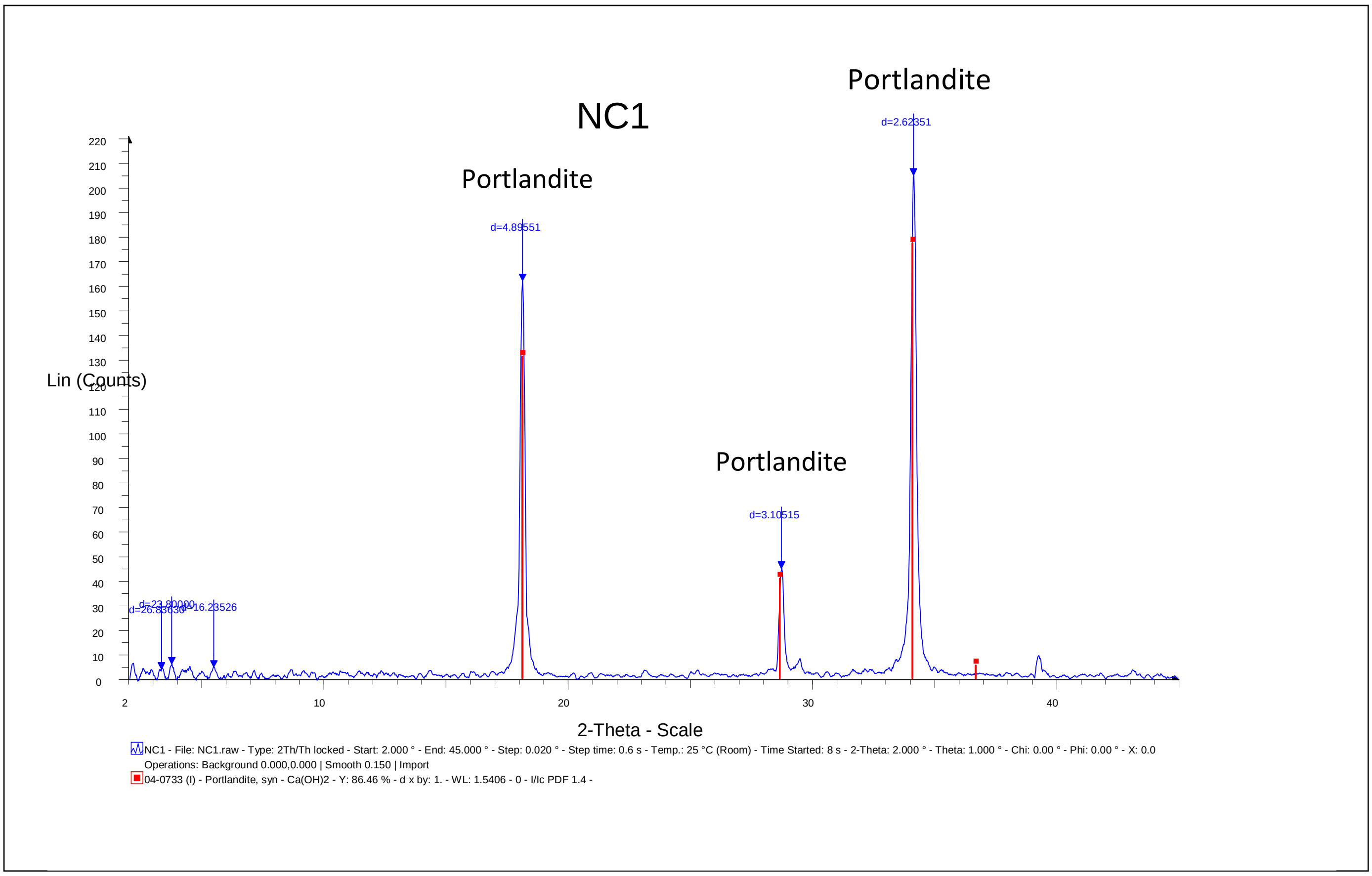

Fig. 17. XRD analysis on NC1 sample.

4.3.6. ESEM observations

The EDAX analysis confirmed the XRD analysis with bands, next to oxygen and platinum bands, characterized by the presence of Ca.

NC1 sample

The unconfined sample is in the form of powder, hard to stick on the pad and difficult to be metallized. The porosity (Fig. 18 (a)) is very high. The grains are generally anhedral, rarely euhedral. They have a size of ± 1 to 5 microns (Fig. 18 (b)).

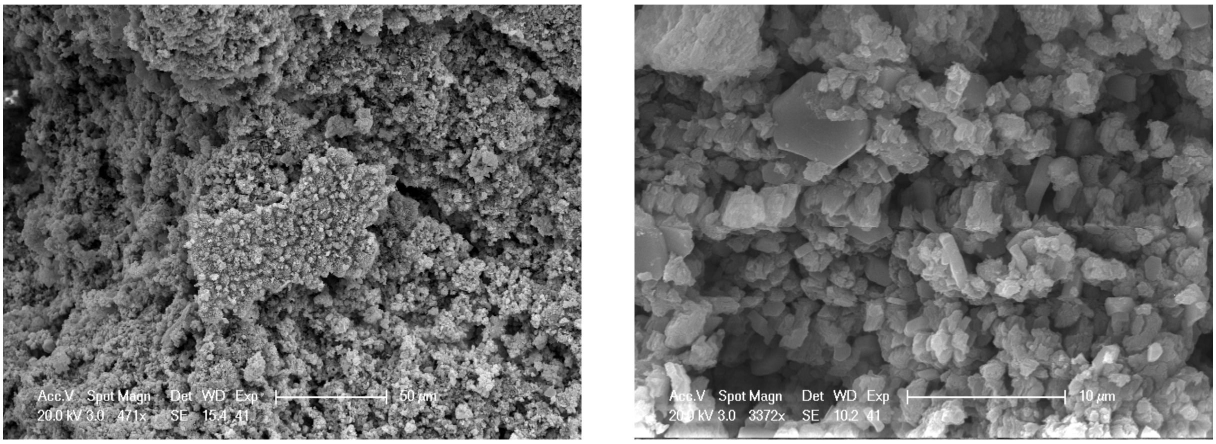

(a) (b)

Fig. 18. ESEM observations on NC1 sample.

C110 sample

The sample shows expansion cracks (Fig. 19 (a)). As in the periphery than in the center of the sample, small euhedral crystals are observed; they attest that there was free space for them for growing and adopting their own crystalline form. The crystals are associated with very small needles blooms (Fig. 19 (b)). The size of portlandite crystals ranges from ± 0.1 to 5 microns.

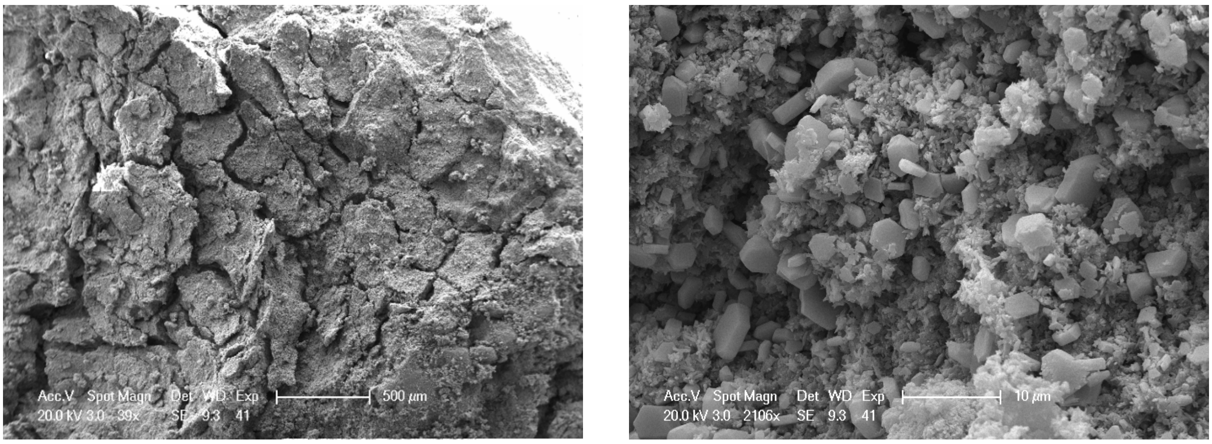

(a) (b)

Fig. 19. ESEM observations on C110 sample.

C115 sample

Like for sample C110, the edge of the core is characterized by the presence of expansion cracks. As in the periphery than in the center, small euhedral crystals are visible (Fig. 20 (a)), which attest about the free space that has existed around them for developing and adopting their crystalline shape. The size of portlandite crystals ranges from ± 2 to 5 microns (Fig. 20 (b)).

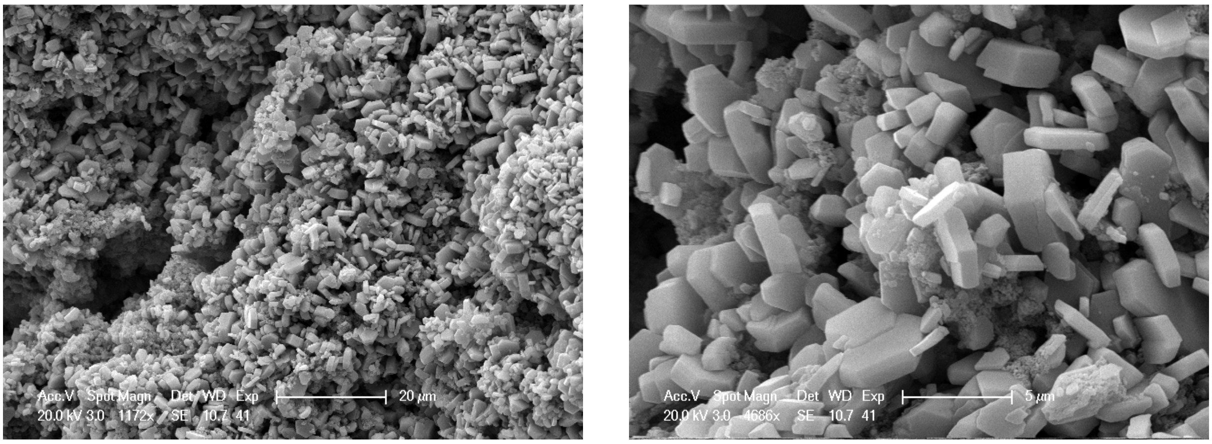

(a) (b)

Fig. 20. ESEM observations on C115 sample.

C120 sample

The puck taken from the sample is very dense. It is cut in the core using an instrument that has left its mark: the wall of the core is regular and detached without tearing (Fig. 21 - sample C120). Anhedral grains are joined and the porosity is low (Fig. 21 (a)). The grain size is about 1 micron (Fig. 21 (b)).

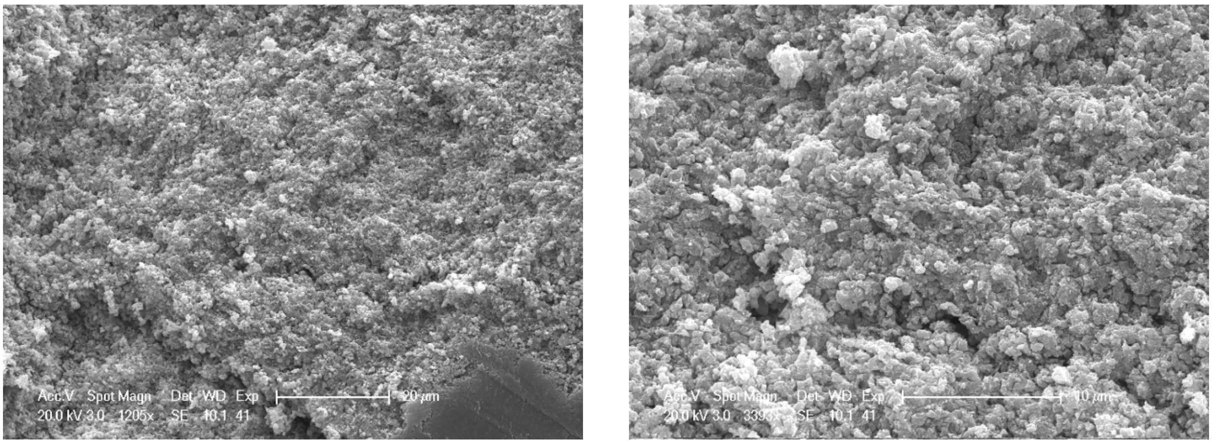

(a) (b)

Fig. 21. ESEM observations on C120 sample.

4.8. Comparisons and analysis of observations

At a low magnification (Fig. 22), two samples show common features (the expansion cracks): C110 (Fig.19 (a) and C115 (Fig.22 (b)). The unconfined NC1 sample (Fig.22 (a)) is in powder form while C120 appears to be more massive (Fig.22 (c)).

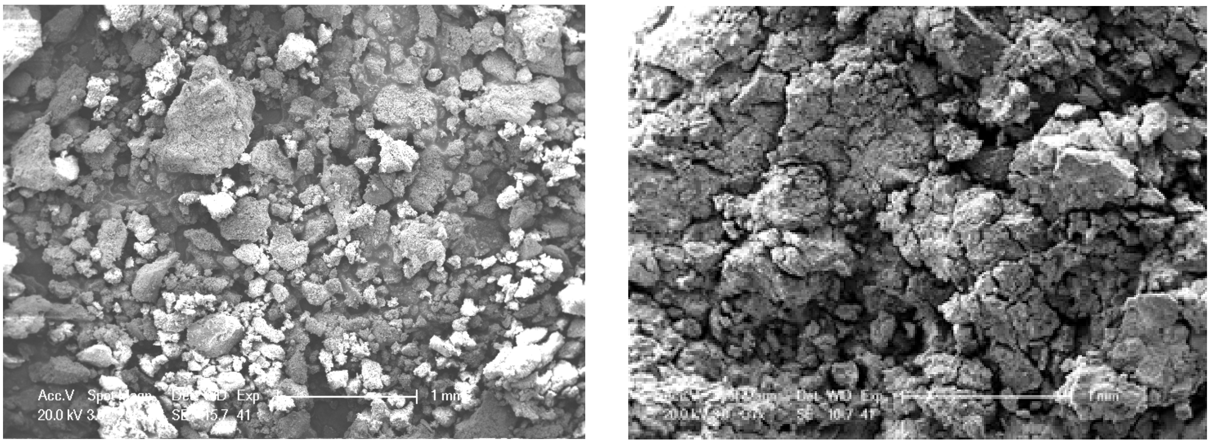

(a) NC1 (b) C115

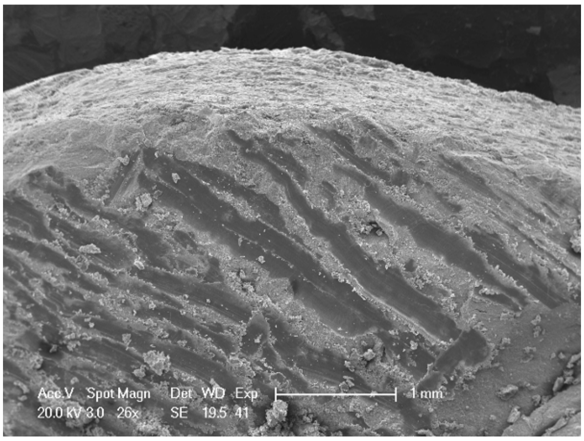

(c) C120

Fig. 22. Comparison of the samples under ESEM (low magnification).

At a higher magnification (1000x to 3000x), even if NC1 (Fig.18 (b)), C110 (Fig.19 (b)), C115 (Fig.20 (b)) samples are similar in grain size, this is not the case with regard to their crystallinity: only C110 and C115 are characterized by the presence of euhedral crystals (Fig. 23). Grain size is finer for sample type C120.

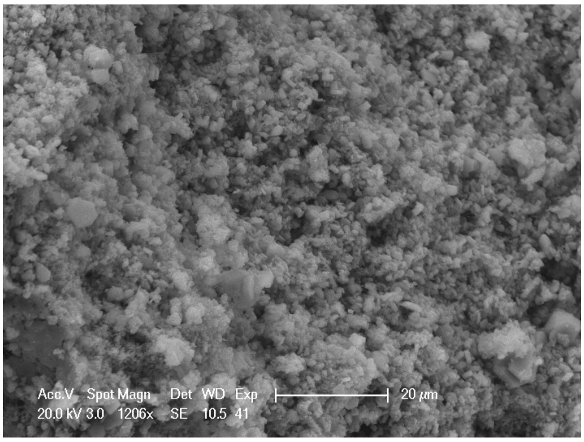

(a) NC1

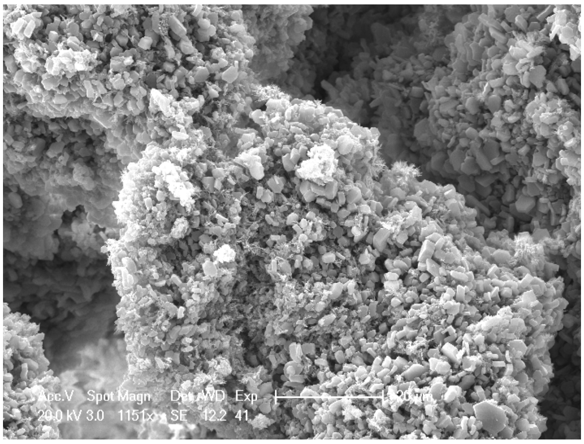

(b) C110

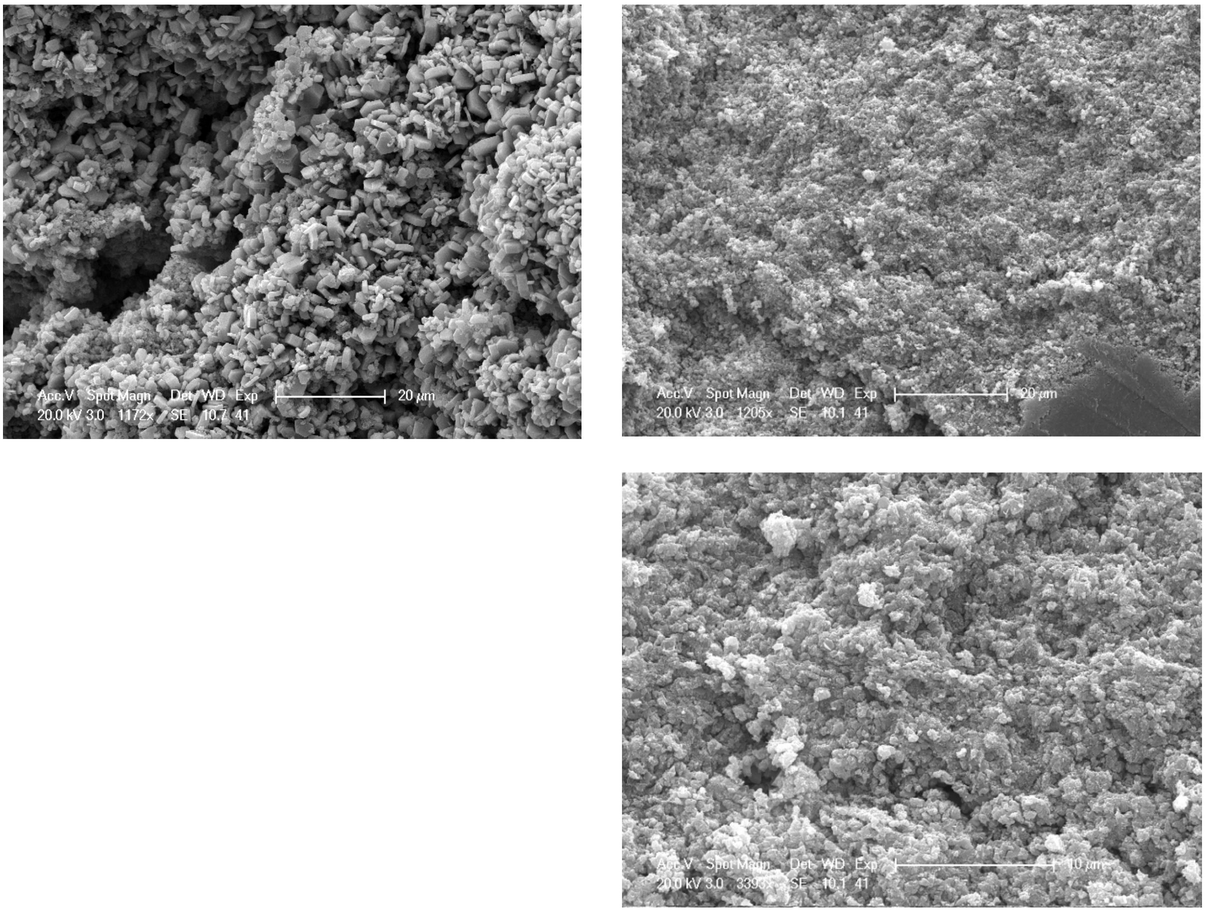

(c) C115 (d) C120

Fig. 23. Comparison of the samples under ESEM (high magnification).

The scanning electron microscopy allowed observing the structures of lime processed under various conditions of confinement, both on site and in the laboratory. The comparison of samples generated in the laboratory shows the difference between unconfined and confined, and, for confined samples, the evolution of structures versus rates of expansion. Structure and porosity may be compared with the densities of cylinders (Table 6).

5. Conclusions

A simple model based on the theory of elasticity, on duly validated experimental data and on reasonable engineering judgement has been derived to estimate the consequences of the presence of hydrated lime nodules from quicklime on the mechanical characteristics of structural concrete and on the risk of occurrence of pop-outs likely to influence concrete durability. By exploiting this simple model, the following conclusions can be drawn:

- for the range of parameters that have been selected, the pressure developed at the interface between the concrete and the hydrated nodule varies from 6 to 60 MPa. The most probable value is of the order of 20 MPa;
- the area of influence of a nodule is of the order of 2 to 3 times its diameter;
- no local crushing of concrete in the vicinity of a nodule is to be considered. If such a crushing would anyway occur, it would only affect a very limited zone around the nodule with no impact on the overall mechanical properties of the concrete;
- a micro-cracked zone is likely to develop around the nodule under the conjunction of unfavourable conditions. The diameter of this cracked region could be at most of the order of 230 % of the diameter of the nodule and its impact on the strength of the concrete at the macroscopic level is proven as negligible;
- for the most probable values of the swelling pressure, the minimum concrete cover thickness allowing the prevention of the pop-out phenomenon is of the order of half the diameter of the inclusion. In other words, under the assumptions considered in this study, no nodule located at a depth of more than half its diameter should cause pop-out even when hydrated;

The following conclusions can be drawn from the experimental program:

- hydration of quicklime in a confined environment, leads to the production of completely hydrated portlandite nodules;
- hydrate formed in a confined environment occupies the available volume and, in present cases, may reach very high densities (average value = 1.55 g/cm^3);

- the rate of volume expansion of the quicklime, depending of the free volume, is very low (average 23% expansion) compared to an unconfined and is the result of a non-full confinement;
- in the case of a fully enclosed environment (case of lime nodules trapped in a concrete structure), the density of the hydrate may reach up to 1.84 g/cm^3, which is still under 2.24 g/cm^3 (absolute and therefore maximum density);
- pop-out appear in the test conditions for depths less than or equal to 0.5 times the initial diameter of the nodule of lime;
- no internal cracking is observed in the concrete blocks;
- when confinement is maximal, anhedral grains are joined and the porosity is low; however, when space around nodules was available, porosity is large and grains shape is euhedral.

Finally, laboratory tests clearly show that the depth of confinement is the most important factor for explaining pop-out and free lime expansion. Moreover, just the near-to-surface layer is affected by the risk of pop-out: when the nodule is under the concrete surface, surrounding concrete is sufficiently resistant to confine nodule and avoid explosion.

Under the worst case scenarios in combined terms of swelling pressure and concrete strength, the minimum thickness necessary to prevent the pop-out phenomenon is of the order of two times the diameter of the inclusion. In other words, even under these extremely unfavourable assumptions, no nodule located a depth of more than 2 times its diameter should cause pop-outs.

References

[1] C. Plinius Secundus (maior), Natural history, translation from Latin by E. Littré (2nd Tome), Paris, 1850.

[2] Ph. Dumont, Use of lime in construction, CERES 99/1 (University of Liège, Belgium), 1999 (*in French*).

[3] J.A.H. Oates, Lime and limestone. Chemistry and technology. Production and uses, Wiley-VCH verlag GmbH, Weiheim, 1998.

[4] R.S. Boynton, Chemistry and Technology of Lime and Limestone, 2nd Edition, New York : Wiley & Sons, 578 pages.

[5] S. Chatterji, Mechanism of expansion of concrete due to the presence of dead burnt CaO and MgO, Cem. Concr. Res. 25(1) (1995) 51-56.

[6] M.H. Lee, J.C. Lee, Study on the cause of pop-out defects on the concrete wall and repair method, Constr. Buildg. Mat. 23(1) (2009) 482-90.

[7] G.M. Idorn, Expansive mechanisms in concrete, Cem. Concr. Res. 22 (1992) 1039-1046.

[8] A. Verhasselt, Industrial by-products for the design of bonded layers in foundations: blast furnace slags, iron slags and fly ashes, Belgian Road Research Center Publication, CR 33/91 (1991) (*in French*).

[9] F. Choquet, Laboratory study for the valorization of iron slags and blast furnace slags in road engineering, Belgian Road Research Center Publication, CR 22/84 (1984) (*in French*).

[10] M. Deng, D. Hong, X. Lan, M. Tang, Mechanism of expansion in hardened cement pastes with hard-burnt free lime, Cem. Conc. Res. 25 (2) (1995) 440-448.

[11] L. Mun-Hwan, L. Jong-Chan, Study on the cause of pop-out defects on concrete wall and repair method, Constr. Bldg. Mat. 23(1) (2009) 482-490.

[12] B. Chiaia, A. Fantilli, G. Ferro and G.Ventura, Modeling the CaO hydration in expansive concrete, Computational Modelling of Concrete Structures (Bicanic et al. eds), CRC Press (2010) 441–449.

[13] H. Shi, L. Yuan, Theoretical and experimental research on expansive stress in hardened cement paste, Advances in Concrete Research 4 (2004) 155-160.

[14] C.F. Dunant, K.L. Scrivener, Effects of uniaxial stress on alkali–silica reaction induced expansion of concrete, Cement and Concrete Research 42 (2012) 567–576.

[15] Faury J., Concrete : influence of inert components – Requirements for a better design, Dunod Ed., Paris (1942) (*in French*).

[16] Dreux G., New guide for concrete, 7th edition, Eyrolles Ed., Paris (1995) (*in French*).

[17] R. D. Hooton, A. M. Ramezanianpur, R. M. Ahani, U. Schutz, Durability of Portland Limestone Cement Concrete, International congress on Durability of Concrete. ICDC 2012, Trondheim, Norway (10p.).

[18] B. Chiaia, A. Fantilli, G. Ventura, A chemo-mechanical model of lime hydration in concrete structures, Constr. Bldg. Mat. 23 (2012) 308-315.

[19] S. Timoshenko and J. N. Goodier, Theory of Elasticity, 2nd Edition, McGraw-Hill Book Company, 1951.

[20] K. Van Baelen, Carbonation of lime mortars and its effect on historical structures, PhD thesis, Catholic University of Leuven (KULeuven), 1991 (*in Dutch*).